Atmospheric Array Loss Statistics Derived from Short Time Scale Site Test Interferometer Phase Data

David D. Morabito* and Larry R. D'Addario†

ABSTRACT. — NASA is interested in using the technique of arraying smaller-diameter antennas to increase effective aperture to replace the aging 70-m-diameter antennas of the Deep Space Network (DSN). Downlink arraying using the 34-m-diameter and 70-m-diameter antennas is routinely performed. Future scenarios include extending the technique to uplink arraying where a downlink signal may not be available. Atmospheric turbulence causes decorrelation of the arrayed signal, and becomes more severe at higher frequencies such as at the uplink allocations near 34 GHz and 40 GHz. This article expands the study initiated in a previous article that focused on average array loss statistics extracted from Site Test Interferometer (STI) data. In that study, cumulative distributions of the annual and monthly expected phasing loss were derived from STI data collected at the Goldstone and Canberra DSN complexes. For a two-element array, the *average* array loss cannot exceed 3 dB. This article considers the *instantaneous* (short time scale) array loss that sometimes exceeds 3 dB for a two-element array. We also consider cases of three-element arrays, which behave somewhat differently. The short time scale statistics of array loss at 7.15 GHz and 34.5 GHz are compared against the average array loss statistics for the best-case and worst-case weather months for the Goldstone and Canberra DSN sites.

I. Introduction

NASA is investigating the use of arraying smaller-diameter antennas to replace aging larger-diameter antennas of the Deep Space Network (DSN). Downlink arraying is routinely performed by the DSN for certain missions. It is desired to extend the technique to uplink arraying (or downlink arraying where a strong reference signal may not be available). Atmospheric turbulence causes degradation of the arrayed signal, and worsens with increasing frequency. NASA is currently characterizing atmospheric effects at all DSN complexes using Site Test Interferometers (STIs). The STIs at the Goldstone and Canberra DSN complexes have been operating for several years. The Madrid STI data collection began in August 2013.

* Communications Architectures and Research Section.
† Tracking Systems and Applications Section.

The research described in this publication was carried out by the Jet Propulsion Laboratory, California Institute of Technology, under a contract with the National Aeronautics and Space Administration.

Preliminary studies of array loss inferred from STI data acquired at Goldstone and Canberra were reported previously [1,2]. These articles provide statistics of atmospheric decorrelation that enable flight projects or preflight mission designers to statistically account for this effect in the design of an arrayed telecommunications link. The annual and monthly cumulative distributions of the zenith delay RMS have been derived from the data acquired by the STIs. These delay RMS statistics were mapped into two-element or three-element average array loss at the DSN uplink frequencies of X-band (7.15 GHz) or Ka-band (34.5 GHz) and at an elevation angle of 20 deg for selected array configurations at the Goldstone and Canberra DSN sites [1].

This article discusses the atmospheric effects on arraying, including the procedures used to map STI phase delay measurements into array loss (Section II). A comparison of average array loss (derived from STI RMS delay over 10-min intervals) with instantaneous array loss (derived from individual STI phase delay estimates at 0.1 s time resolution) is presented in Section III for selected array configurations. Finally, we offer some conclusions in Section IV.

II. Estimation of Atmospheric Effects on Arraying

For single antennas, the principal atmospheric-related effects on telecommunications link performance are the atmospheric attenuation and noise temperature increase resulting from oxygen, water vapor, clouds, and rain. These effects are described and their magnitudes documented in the *DSN Telecommunications Link Design Handbook* [3–6].

For phased arrays, an additional loss occurs when the phase alignment is not accurate. Even if the instrumental alignment is perfect, random misalignments are introduced by turbulence in the atmosphere. For a downlink array where a sufficiently strong signal is available, it is possible to measure and correct for this effect during signal processing. For an uplink array (or a downlink array without a strong reference signal), correction is not feasible, so the expected loss should be accounted for in the link budget using tables such as those presented in [1].

The STIs deployed at the Goldstone, Canberra, and Madrid DSN complexes provide measurements of the phase delay difference on baselines ~200 m using a signal emitted from a geostationary satellite. These measurements have a time resolution of 0.1 s and an accuracy of better than 0.5 ps, which are sufficient to capture most of the delay fluctuations caused by atmospheric turbulence. Details of the instrument design were given previously [7,8]. We use the STI measurements to derive statistics of the delay fluctuations (such as the variance over 10-min intervals). Using well-established models [1,2], similar statistics can be derived for different baseline lengths and elevation angles. The expected phase alignment loss for a particular array configuration at the same site can then be predicted.

The average two-element array loss for a delay RMS value of $\sigma_{\Delta\phi}$ can be shown [9] to be

$$Array\ Loss\,(dB) = -10\log\left[\left(\tfrac{1}{2}\right)\left(1+e^{-\sigma^2_{\Delta\phi}/2}\right)\right] \tag{1}$$

where $\sigma_{\Delta\phi}$ is the RMS of $\Delta\phi$, the phase difference between the two antennas in the STI, evaluated over 10-min intervals.

The RMS delay fluctuations over 10-min intervals were measured by the STIs at Goldstone and Canberra and were converted to expected array loss in this manner. This method provides a good estimate of the expected (mean) array loss in most cases, but the instantaneous loss can be larger or smaller. As Equation (1) shows, the expected loss for a two-element array cannot exceed 3 dB.

At 34 GHz, the 3-dB limit is sometimes approached during the most turbulent months for Goldstone and Canberra [1]. Array loss values exceeding 3 dB are possible at short time scales, thus calling into question the usefulness of this method at high frequencies. Therefore, array loss statistics on short time scales will be examined and compared against the average array loss statistics. The formula for calculating average array loss [Equation (1)] was derived assuming that the phase difference $\Delta\phi$ is normally distributed with mean of zero and standard deviation of $\sigma_{\Delta\phi}$ [9]. This assumption is formally accurate, but whereas $\Delta\phi$ is nonstationary (varying diurnally, seasonally, and with local weather), its samples over an extended time interval may not be normally distributed. However, over sufficiently short time intervals such as 10-min blocks, there is evidence that the samples approach a normal distribution, and that the use of average array loss statistics should provide a reasonable approximation. We therefore compute the average array loss separately for each 10-min block, and perform intercomparisons between instantaneous and average array loss statistics using data taken over one quiet month (best-case weather) and one active month (worst-case weather).

To estimate instantaneous array loss, we take the STI-measured delay difference at each 0.1-s data point, convert to phase difference at the array's frequency, adjust to the elevation angle of the array, and finally adjust to the antenna spacing of each baseline in the array (see Section II.C in [1]). This gives the estimated phase difference $\Delta\phi$ for that baseline. For a two-element array (single baseline), the array loss is then

$$Array\ Loss\,(dB) = -10\log\left[0.5\left(1+\cos\left(\Delta\phi\right)\right)\right]. \tag{2}$$

This produces a more accurate but more tedious method in estimating array loss. We therefore only perform the analysis for the months with the best weather and the worst weather for both Goldstone and Canberra. As shown in Section III, the cumulative distribution of this estimated instantaneous loss is comparable to that of the 10-min average loss when both are small, but they differ when the loss is high.

We also construct the average array loss for a three-element array, assuming that the phase pair estimates are Gaussian and stationary over 10-min intervals as

$$Array\ Loss\,(dB) = -10\log\left\{\tfrac{1}{9}\left(3+2e^{-\sigma^2_{\Delta\phi 12}/2}+2e^{-\sigma^2_{\Delta\phi 13}/2}+2e^{-\sigma^2_{\Delta\phi 23}/2}\right)\right\} \tag{3}$$

where the $\sigma^2_{\Delta\phi ij}$ are the RMS phase estimates over 10-min blocks for baselines consisting of elements i and j [9].

The average array loss for a three-element array reaches a maximum of –10 log(3/9) = 4.7 dB (versus 3 dB maximum for a two-element array) for sufficiently large values of $\sigma_{\Delta\phi ij}$ in Equation (3).

For a three-element array, the instantaneous array loss is given by

$$Array\ Loss\,(dB) = -10\log\left\{\tfrac{1}{9}\left(3 + 2\cos\Delta\phi_{12} + 2\cos\Delta\phi_{13} + 2\cos\Delta\phi_{23}\right)\right\} \qquad (4)$$

where $\Delta\phi_{ij}$ is STI delay difference adjusted to estimate the phase difference for the array baseline consisting of elements i and j [9].

The formulation presented in this section calculating array loss will now be applied to specific two-element and three-element arrays at Goldstone and Canberra for frequencies of 7.15 GHz and 34.5 GHz.

III. Comparison of Average and Instantaneous Array Loss

The average array loss estimates presented in [1] are based on STI data acquired at Goldstone and Canberra during 2011, 2012, and 2013. They include 32 months of Goldstone data from January 2011 through August 2013, and 28 months of Canberra data from May 2011 through August 2013 [1].

Both Canberra and Goldstone STIs are three-element instruments. Data acquired show that the delay RMS statistics from all baselines are very similar after accounting for difference in baseline lengths. Therefore, for the two-element analysis we have chosen to use the statistics from only the east–west baseline at each site with the expectation that the statistics will not vary significantly with the inclusion of data from the other two baselines [7]. For three-element arrays, we make use of the data from all three STI baselines in calculating instantaneous array loss, assuming a hypothetical array of antennas occupying the locations of the three STI elements.

A. Delay RMS Statistics

Several years of STI data are now available for the Goldstone Apollo and Canberra stations. The monthly and yearly statistics of the zenith RMS delay were generated for each month of STI data and were presented in [1] in a format similar to the single-antenna atmospheric attenuation and noise temperature tables in the *DSN Telecommunications Link Design Handbook* [3]. Figure 1 displays the cumulative distribution (CD) of the 10-min RMS zenith delay difference derived from the east–west STI baseline data for each calendar month at the Goldstone DSN site [1]. In Figure 1(a), we see that there is a strong seasonal separation (summer–red to winter–violet) among the curves that is consistent with the Goldstone desert climate being warm and humid during the summer months and cool and dry during the winter months. Figure 1(b) displays the monthly CD curves of zenith delay RMS for Canberra as reported in [1] that also shows a seasonal separation, although not as strong as Goldstone's [see Figure 1(a)].

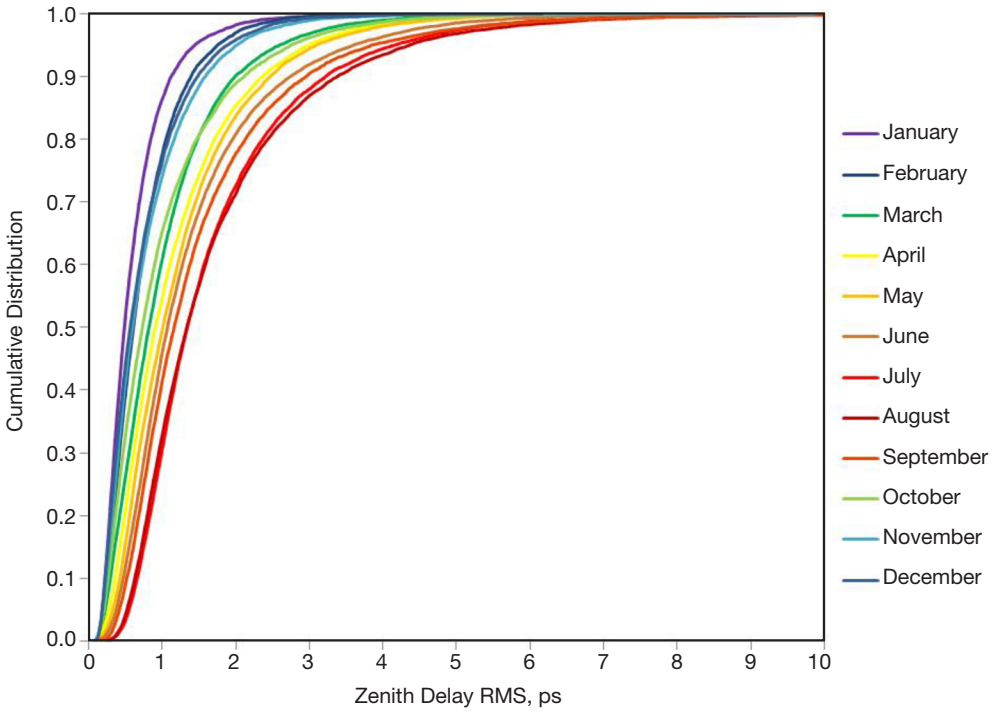

Figure 1(a). Monthly cumulative distribution curves of zenith delay RMS for the Goldstone Apollo east–west STI baseline.

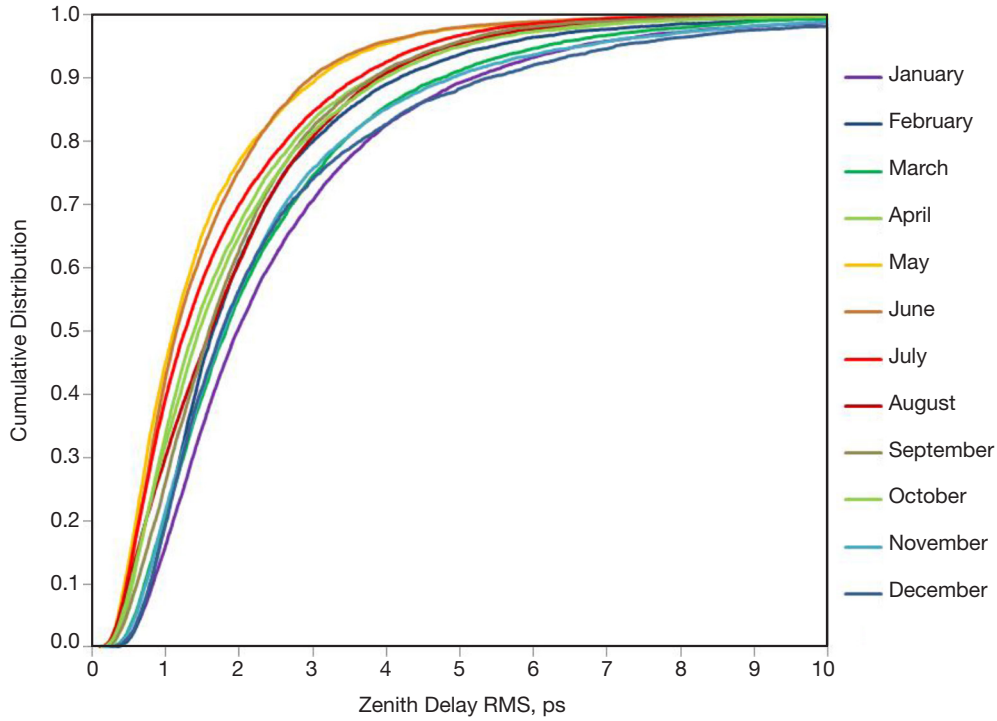

Figure 1(b). Monthly cumulative distribution curves of zenith delay RMS for the Canberra east–west STI baseline.

The delay RMS values presented in [1] were converted to values of array loss for selected existing antenna configurations using the stated procedures. The 3-dB limit was attained at 34.5 GHz for some 10-min intervals in every month at Canberra and for the more turbulent months at Goldstone. It can thus be expected that losses exceeding 3 dB will occur over short intervals of time. Therefore, we will examine estimates of instantaneous array loss statistics for both worst-case and best-case months for both Goldstone and Canberra and compare these against those obtained using the average method discussed in [1].

B. Array Loss Comparison for DSN Two-Element Arrays

Based on unpublished data from downlink array demonstrations using two Goldstone antennas — DSS-25 and DSS-26 — tracking the Cassini spacecraft, the Goldstone Apollo STI data, when adjusted to the conditions of those measurements (baseline projection, elevation angle, frequency), produced RMS phase statistics that were in reasonable agreement with the statistics of the phase differences between DSS-25 and DSS-26 over a wide range of elevation angles and baseline projections. Therefore, we believe that the adjustments in elevation angle and baseline length used to map the STI phase data to the conditions of the two-element DSN arrays have validity.

For Goldstone, we selected the month with the largest RMS delay (August 2012) and the month with the smallest RMS delay (December 2011) for detailed examination. We used the 0.1-s delay time series from the east–west STI baseline of length ~191 m for Goldstone over each month. Each delay sample was adjusted to correspond to a 20-deg elevation angle and the baseline distance of the DSS-25/DSS-26 antenna pair (~302 m) using adjustment factors described in [1]. The samples were then converted to phase at the DSN uplink frequencies of 7.15 GHz and 34.5 GHz and also to estimates of array loss using Equation (2). The resulting array loss cumulative distribution displayed in Figure 2 for 7.15 GHz and in Figure 3 for 34.5 GHz will now be discussed.

We examined the cumulative distribution of the 7.15-GHz DSS-25/DSS-26 array loss estimated from both techniques: (a) average delay RMS over 10-min intervals [Equation (1)], and (b) instantaneous phase delay time series at 0.1 s time sampling [Equation (2)]. The results at 7.15 GHz for both months are displayed in Figure 2. The two August 2012 curves (blue) cross over near 90 percent at ~0.2 dB. The instantaneous array loss (solid blue curve) lies below the average array loss (dashed blue curve) 90 percent of the time, suggesting that the 7.15-GHz average array loss in the tables of [1] provide conservative estimates useful for planning or link studies. Above the 90th percentile (above 0.2 dB array loss), the instantaneous loss is higher than the average loss at a given percentile. The difference in array loss estimates between the two techniques is quite small: less than 0.1 dB up to the 97th percentile. As this applies to the worst-case month of August 2012, such dB differences are expected to be smaller for other months. For the best-case month of December 2011, the two red curves in Figure 2 cross near the 90th percentile at values less than 0.02 dB. The array loss is thus not significant during winter. For all months, the curves of Figure 2 serve as best-case and worst-case bounds. Below the 90th percentile, the tables in [1] thus provide reasonable conservative estimates of array loss at 7.15 GHz.

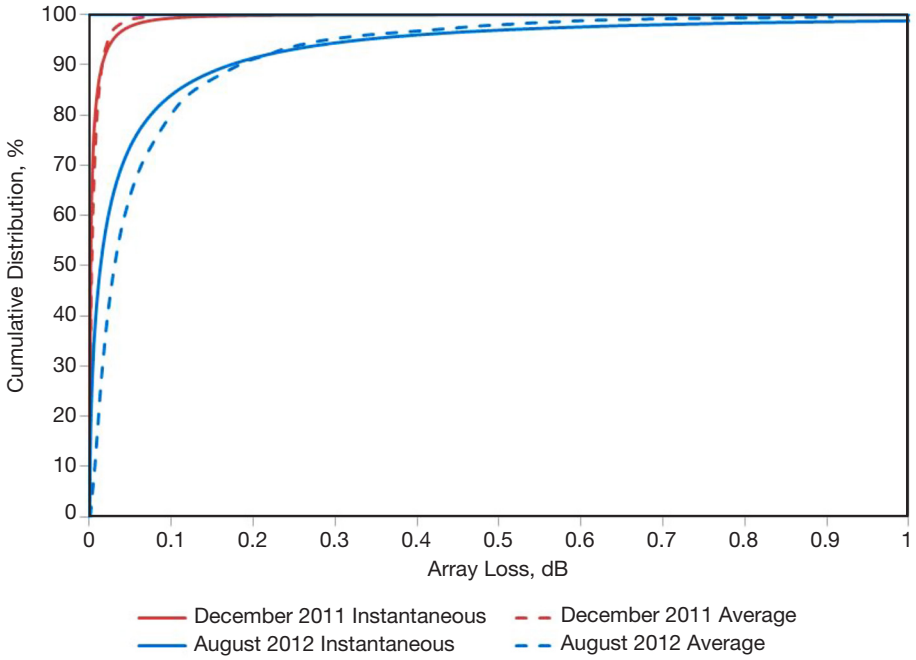

Figure 2. Cumulative distribution of 7.15-GHz array loss for Goldstone DSS-25/DSS-26 at 20-deg elevation angle for August 2012 (blue curves) and December 2011 (red curves) showing both methods: average (dashed) and instantaneous (solid).

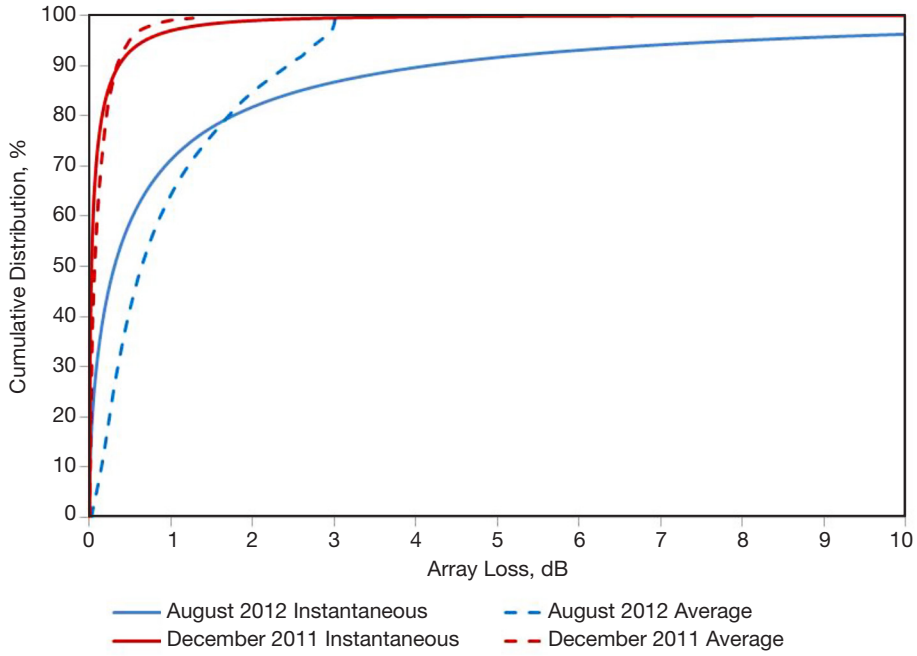

Figure 3. Cumulative distribution of 34.5-GHz array loss for Goldstone DSS-25/DSS-26 at 20-deg elevation angle for August 2012 (blue curves) and December 2011 (red curves) showing both methods: average (dashed) and instantaneous (solid).

Figure 3 displays the results at 34.5 GHz for a 20-deg elevation angle for the DSS-25/DSS-26 array in the same two months. At this frequency, the differences between the two methods are significantly larger. The December 2011 curves cross at the 90th percentile (0.4 dB), so the average loss results of [1] provide a conservative estimate for lower percentile values. The curves for August 2012 cross over at the 78th percentile (1.7 dB). Above this percentile, the average loss deviates greatly from the instantaneous loss, since it cannot exceed 3 dB. Thus, the values in Table 7 in [1] can be treated as upper bounds for percentiles below about 80 percent for August and below 90 percent for most months. Above the 80th percentile, the fades can be severe. The solid blue curve in Figure 3 should provide reasonable upper bounds of array loss at high percentiles for any month of the year. Likewise, the solid red curve in Figure 3 can serve as a best-case lower bound for any month of the year. A complete loss is theoretically possible when the phase difference is 180 deg, as shown by Equation (2).

In practice, during turbulent weather conditions at high frequencies, a single element may be a better choice than a two-element array, even though the latter would on average provide an advantage of nearly 6 dB (for uplink). For arrays of three or more antennas, the probability of deep fades is substantially lower, as will be shown. The performance of a spacecraft receiver in recovering from dropouts due to fades of various depths and time scales should also be considered.

The statistics for the months with the highest delay RMS (December 2012) and lowest delay RMS (June 2013) will be examined for Canberra. The residual phase time series for the east–west baseline (~250 m) was adjusted to refer to a 20-deg elevation angle and the baseline distance of the DSS-34/DSS-35 antenna pair (~302.5 m). Both cases considered the uplink frequencies of 7.15 GHz and 34.5 GHz. The filtered residual phase value at each 0.1-s data point was converted to array loss using the formulation discussed in Section II.

We have examined the cumulative distribution of the 7.15-GHz instantaneous array loss for DSS-34/DSS-35 that could be compared against that of the average array loss (Figure 4). The two curves for December 2012 cross over near 95 percent (0.52 dB). Below 95 percent, the average array loss dominates, suggesting that it can be used to provide conservative estimates. Above the 95th percentile, the instantaneous array loss curve dominates with higher values for a given percentile, and the difference continues to grow above 95 percent. It is thus recommended that the solid blue curve in Figure 4 be used at very high percentiles as an upper bound. This result applies to the worst-case month, as such dB differences are expected to be smaller for other months. For the best-case month of June 2013, the crossover point of the curves occurs near the 90th percentile at ~0.06 dB. The best-case month curves for June 2013 thus show array loss values below 0.1 dB at and below the 90th percentile.

For 34.5 GHz, we see from Figure 5 that the average array loss values provide conservative estimates below the 85th percentile for June 2013 and below ~80 percent for December 2012. Above these percentiles, the solid curves provide best-case and worst-case bounds on array loss over the course of a year. There is a stark difference in the pattern of the December 2012 curves as the 3 dB limit is reached for the average (dashed blue) curve, while the instantaneous (solid blue) curve reaches ~83 percent at 3 dB and continues smoothly to higher array loss values (up to 10 dB at ~95 percent).

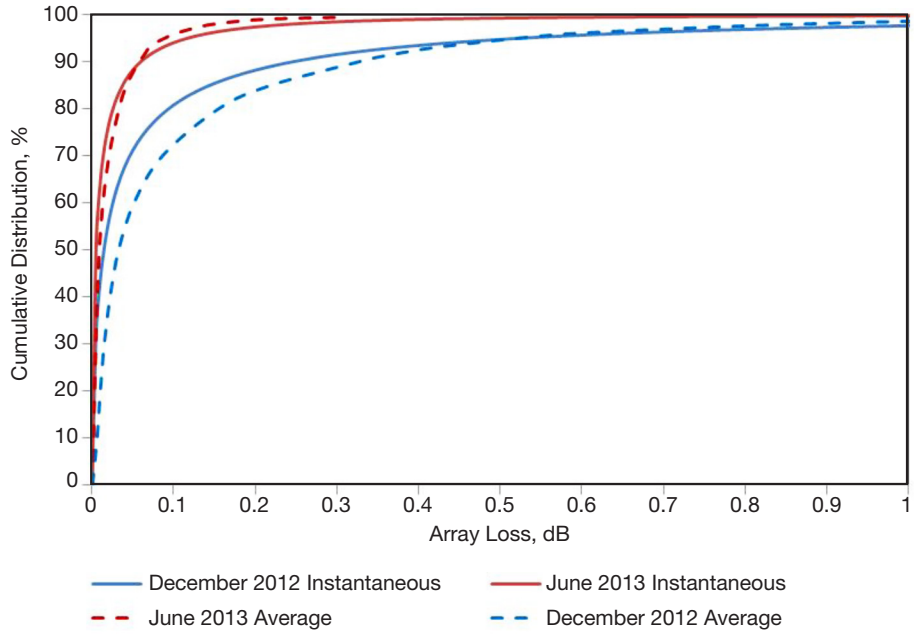

Figure 4. Cumulative distribution of 7.15-GHz array loss for Canberra DSS-34/DSS-35 at 20-deg elevation angle for December 2012 (blue curves) and June 2013 (red curves) showing both methods: average (dashed) and instantaneous (solid).

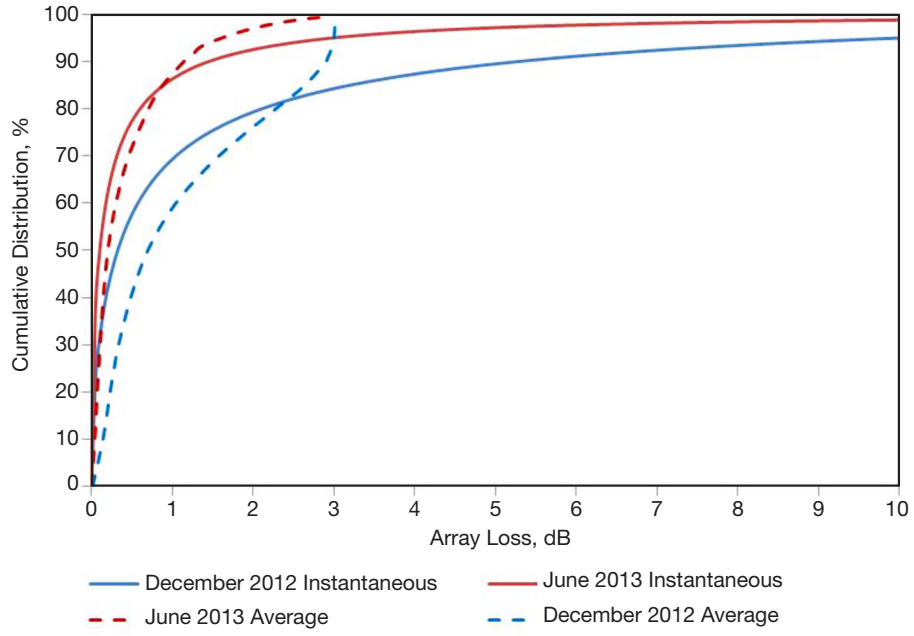

Figure 5. Cumulative distribution of 34.5-GHz array loss for Canberra DSS-34/DSS-35 at 20-deg elevation angle for December 2012 (blue curves) and June 2013 (red curves) showing both methods: average (dashed) and instantaneous (solid).

A fade analysis was performed to gain insight into the average duration and number of events of signal fades extracted from the array loss time series at each frequency band for both worst-case and best-case months at Goldstone. The array loss time series was processed to count the number of fades that exceeded a given threshold and to evaluate their average duration. Figure 6 displays the average fade duration as a function of array loss. The average durations of all fades with thresholds above 1 dB and below 10 dB lie between 1 s and 10 s; above 10 dB the durations become progressively shorter, approaching the sampling limit of 0.1 s near 50 dB. The December 2011 fade durations at 7.15 GHz (red triangles) are between 1.5 and 6 s and there are no data with array loss >2 dB for that month.

The August 2012 fade durations at 7.15 GHz for Goldstone are ~8 s near an array loss of 1 dB and decline to 1 s at 12 dB. The 34.5-GHz fade durations for December 2011 (blue triangles) lie between 1.5 s and 2 s out to 10 dB before declining to lower values. The August 2012 34.5-GHz fade durations (blue squares) lie near 8 s at ~1 dB and decline steadily to lower values as the array loss increases.

Figure 7 displays the number of fade events as a function of fade value for each frequency band and month. The number of events curve for August 2012 at 34.5 GHz (blue squares) dominates at the high array loss values over all other curves, including the 7.15-GHz curve for August 2012. The 7.15-GHz August 2012 curve aligns well with the 34.5-GHz curve for December 2011 at high array loss values >10 dB. The number of events curve for 7.15 GHz for December 2011 shows the fewest events and does not extend beyond the highest fade measured near 2 dB for that month. Thus, one can see that there is about a factor of 100 reduction in number of events from summer to winter at high values of array loss (see Figure 7).

An interesting threshold to consider is 6 dB, which occurs when the two-element array is down to the single-antenna power. In August 2012 at 34.5 GHz, 6 dB is exceeded about 9 percent of the time (Figure 3) or 65 hours. This corresponds to about 40,000 events (Figure 7) of average duration ~7 s (Figure 6). In contrast, the loss is less than 1 dB (5 dB better than a single antenna) 73 percent of the time (Figure 3). Each mission design team must decide whether such a trade-off is worthwhile.

A fade analysis was also performed for Canberra to gain insight into the average duration and distribution of signal fades as a function of array loss at each frequency band for worst-case and best-case months. Figure 8 displays the average fade duration as a function of array loss. The average durations range from subsecond to several seconds depending upon the month and frequency band. It is interesting that at 34.5 GHz, the fade duration signatures as a function of array loss are similar for both the summer month (December 2012) and for the winter month (June 2013), whereas the signatures at 7.15 GHz are very different. The summer month 7.15-GHz fade durations take on longer values (up to 10 s) than the winter month 7.15-GHz curve, which takes on shorter durations (~s) at small array loss values.

Figure 9 displays the number of events as a function of fade value for both frequency bands and both months for the Canberra DSN site. The number of events curve for December 2012 (summer month) at 34.5 GHz dominates over all other curves. At 7.15 GHz, the December 2012 (summer month) curve aligns reasonably well with the June 2013 (winter month) curve.

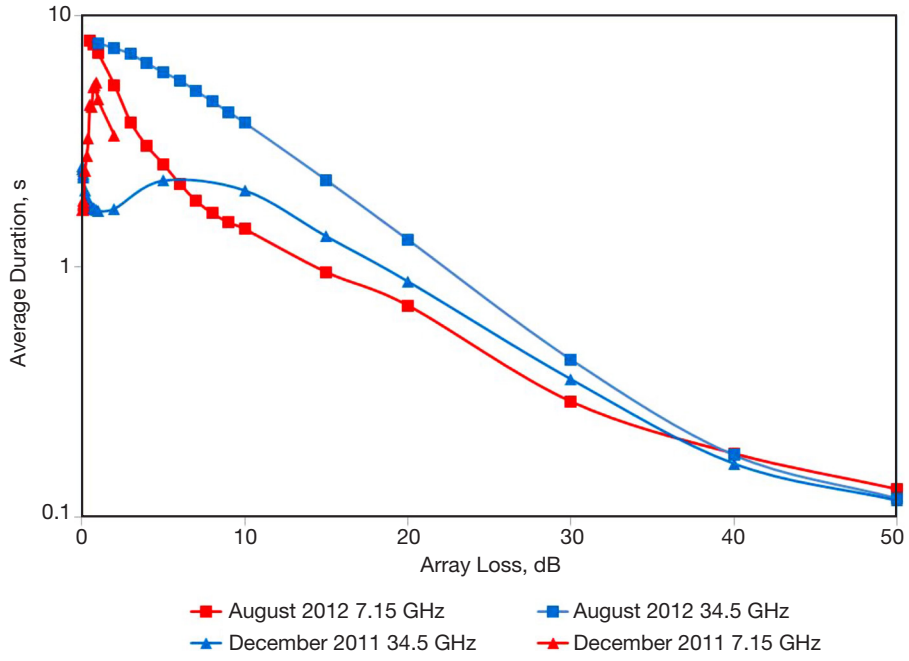

Figure 6. Goldstone STI average fade duration for DSS-25/DSS-26 at 20-deg elevation angle versus fade threshold for worst-case month (August 2012) and best-case month (December 2011) at 34.5 GHz (blue curves) and at 7.15 GHz (red curves).

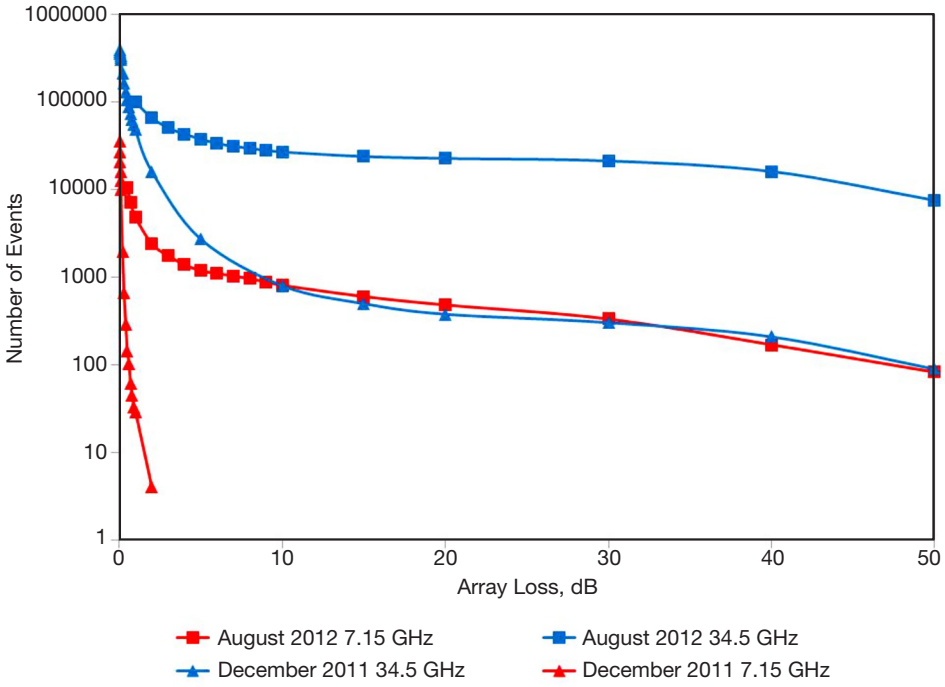

Figure 7. Goldstone STI number of events exceeding threshold for DSS-25/DSS-26 at a 20-deg elevation angle for worst-case month (August 2012) and best-case month (December 2011) at 34.5 GHz (blue curves) and at 7.15 GHz (red curves).

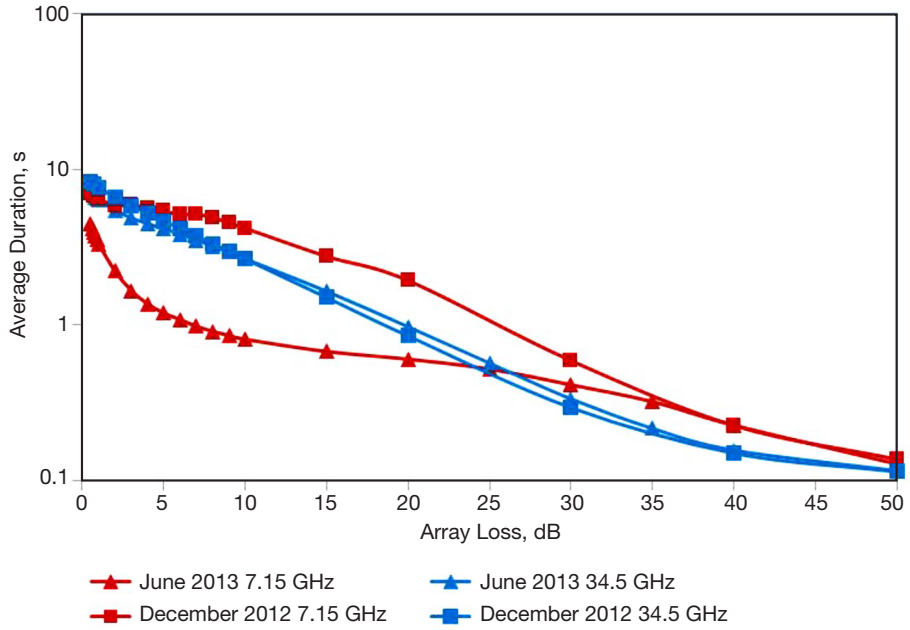

Figure 8. Canberra STI average duration for DSS-34/DSS-35 array versus fade threshold for December 2012 and June 2013 at 34.5 GHz (blue curves) and at 7.15 GHz (red curves).

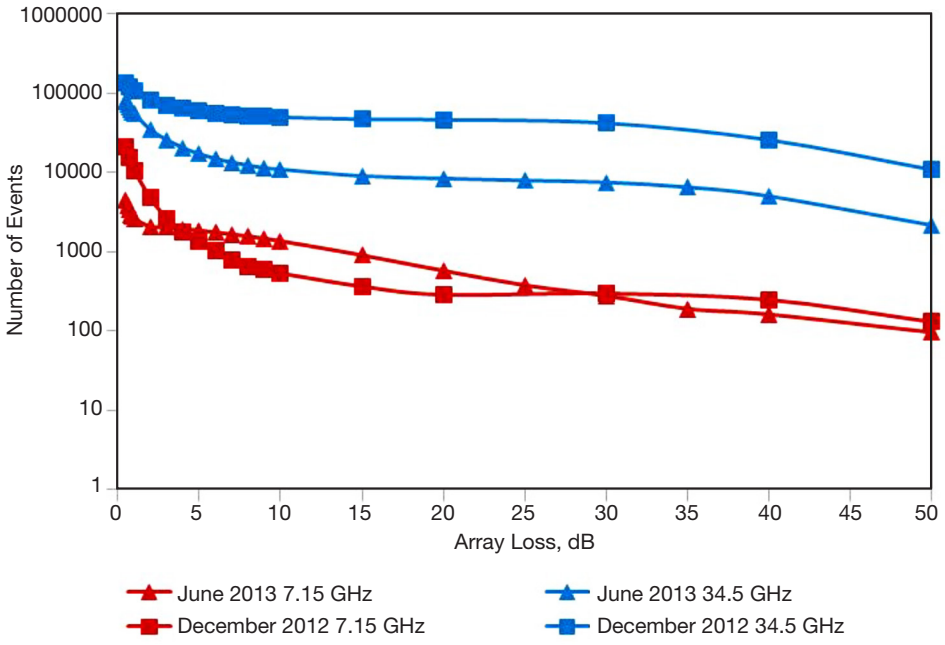

Figure 9. Canberra STI number of events exceeding specified fade threshold for worst-case month (December 2012) and best-case month (June 2013) at 34.5 GHz (blue curves) and at 7.15 GHz (red curves).

We also considered the case of a hypothetical pair of antennas located at the same positions and pointed in the same direction as the STI antennas, so that no adjustments for baseline length or elevation angle are needed. In comparison to the case of the DSS-25/DSS-26 array at a 20-deg elevation angle and an element separation of 302 m, the array loss values for the hypothetical case at a given percentile is significantly lower because the elevation angle is higher (47 deg) and the element spacing is shorter (191 m). The crossover points of the average and instantaneous loss curves are similar to those of DSS-25/DSS-26 in Figure 2. Similar results were achieved for the Canberra hypothetical baseline case. The details of the hypothetical two-element case will not be presented. They will, however, be qualitatively compared against those of the hypothetical three-element case, to be discussed next.

C. Array Loss Statistics for a Hypothetical Three-Element Array

The validity of adjusting the instantaneous STI delay measurements for elevation and baseline length to that of a three-element DSN array is yet to be established, unlike adjustments of the RMS delay or delay measurements for the two-element DSN array case. We therefore assume that we have an array consisting of three 34-m-diameter antennas, each located at an STI element site and pointed at the STI elevation angle to its geostationary satellite. We again consider the best-case month (December 2011) and the worst-case month (August 2012) for the Goldstone Apollo site. We then use the STI delay difference measurement at each 0.1-s sample for each of the three baselines to calculate instantaneous array loss using Equation (4) and then construct its cumulative distribution for each case. We also construct the average array loss for each month in the usual manner for comparison using Equation (3).

Figure 10 displays the cumulative distributions of three-element array loss at Goldstone for 7.15 GHz at 47-deg elevation angles for both December 2011 (best-case month) and August 2012 (worst-case month). The array loss for December 2011 lies below 0.02 dB for percentiles below 90. The instantaneous and average curves for August 2012 align up very well given the low values of array loss.

Figure 11 displays the cumulative distributions of three-element array loss for Goldstone at 34.5 GHz at the 47-deg STI elevation angle for both December 2011 (best-case month) and August 2012 (worst-case month). The average array loss at 34.5 GHz for August 2012 can be seen to reach the theoretical maximum of 4.7 dB in Figure 11.

We also consider the case of a three-element hypothetical array for Canberra in which the antennas occupy the locations of the STI elements and no adjustments are made other than those for frequency. Figures 12 and 13 show the array loss figures for this case with 250 m element separation on each baseline at the Canberra STI elevation angle of 48.25 deg, for 7.15 GHz and 34.5 GHz, respectively.

From Figure 12, the 7.15-GHz array loss for December 2012 lies below 0.2 dB for percentiles below 90. The instantaneous and average curves for June 2013 align up very well given the very low values of array loss.

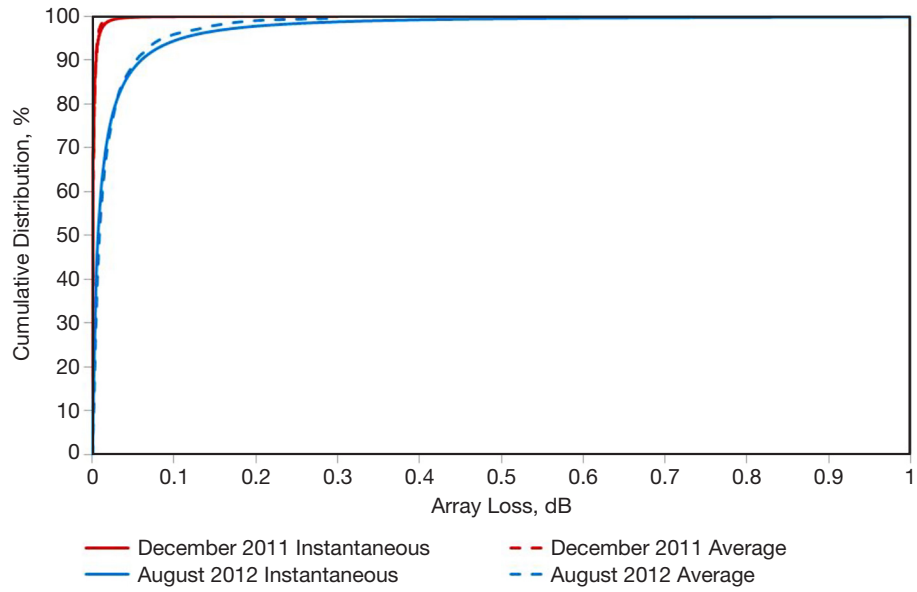

Figure 10. Cumulative distributions of three-element array loss at Goldstone for 7.15 GHz at 47-deg elevation angle for December 2011 (best-case month) and August 2012 (worst-case month) showing both methods: average and instantaneous array loss.

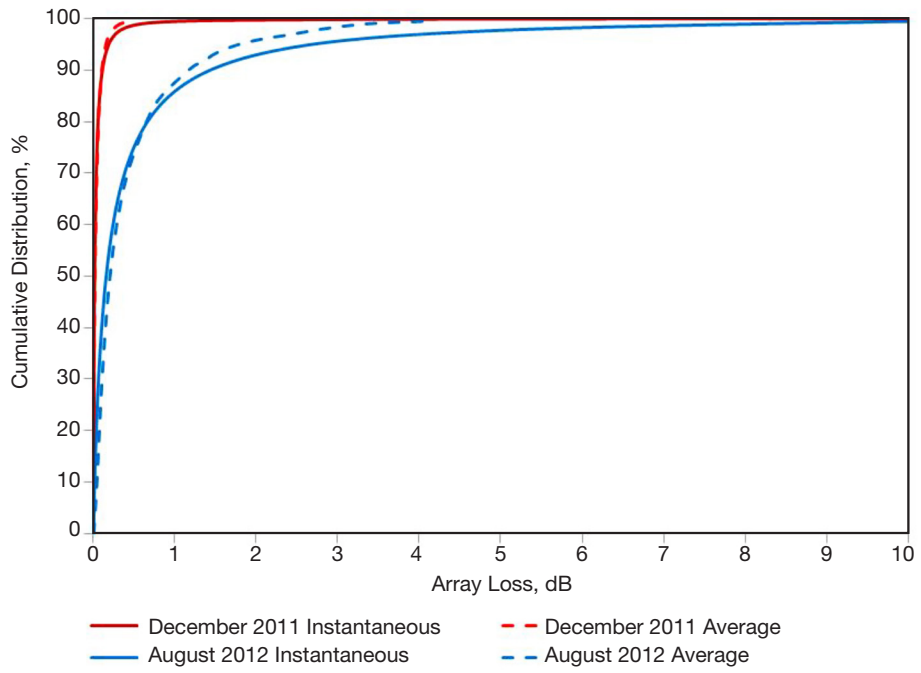

Figure 11. Cumulative distributions of three-element array loss for Goldstone at 34.5 GHz at 47-deg elevation angles for December 2011 (best-case month) and August 2012 (worst-case month) showing both methods: average and instantaneous array loss.

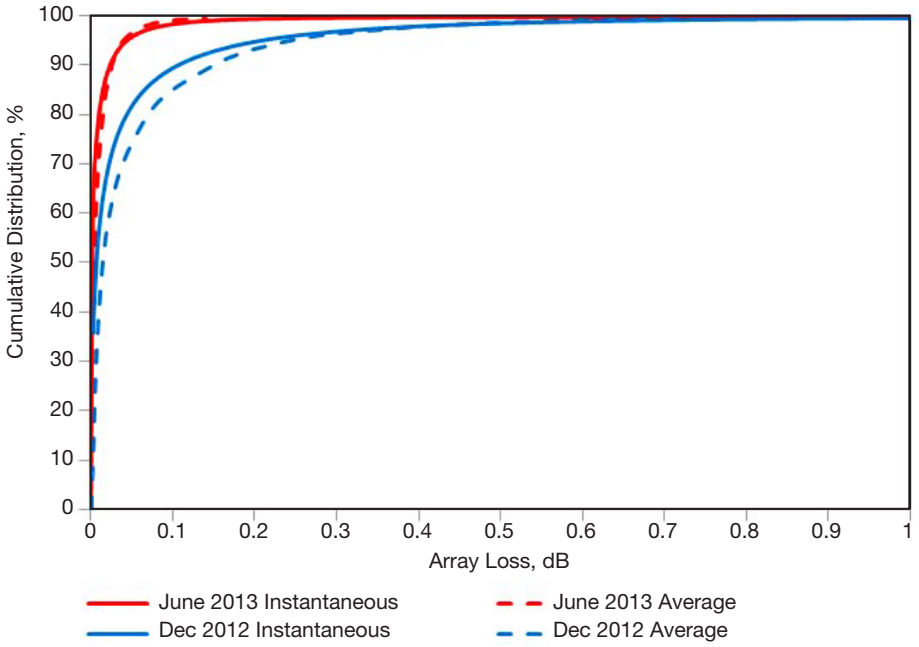

Figure 12. Cumulative distribution of three-element array loss at Canberra for 7.15 GHz at 48.25-deg elevation angle for December 2012 (worst-case month) and June 2013 (best-case month) showing both methods: average and instantaneous array loss.

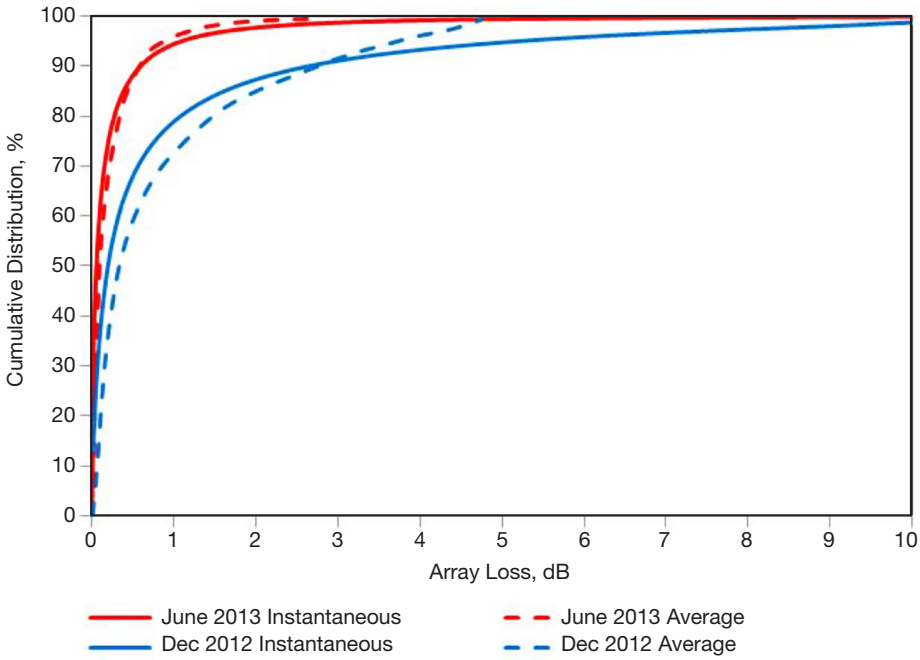

Figure 13. Cumulative distribution of three-element array loss at Canberra for 34.5 GHz at 48.25-deg elevation angle for December 2012 (worst-case month) and June 2013 (best-case month) showing both methods: average and instantaneous array loss.

In Figure 13, the 34.5-GHz average cumulative distribution curve is observed to reach the 4.7-dB theoretical limit. The 90 percent array loss for December 2012 lies near 2.8 dB for both curves where they cross over each other. However, at 97 percent, the average array loss is 4.3 dB while the instantaneous array loss is 7.4 dB, which is much higher but more realistic.

We now examine average durations and fade counts for the three-element array for Goldstone. From Figure 14, we see that for fade values of less than 10 dB, the average durations typically run between 1 s and 10 s, whereas when the fade depths approach higher values, the time scales become subseconds, reaching the sampling limit of 0.1 s for both Ka-band curves. Almost all of the 7.15-GHz average fade durations lie between 1 s and 10 s. An interesting point regarding the three-element average durations: they appear to exhibit a higher rate of decrease and reach the 0.1-s sampling limit sooner (Figure 14) than those of the two-element hypothetical case (which is similar to the DSS-25/DSS-26 two-element case shown in Figure 6). Figure 15 displays the number of fades as a function of fade depth, where we see steep decreases for the 34.5-GHz cases relative to what was observed for the two-element array cases. We also see that the December 2011 34.5-GHz array loss cuts off at 25 dB for the three-element case (Figure 15) versus 40 dB for the hypothetical two-element case (not shown). We also see the effect of the rapid decrease for the 7.15-GHz August 2012 curve cutting off at 8 dB (Figure 15) versus the curve continuing to 50 dB for the hypothetical two-element case (not shown).

There was very little change in the average durations for Canberra at small values of array loss (Figure 16) for the three-element array relative to that of the two-element array case (not shown). However, the three-element average durations decrease with array loss until they reach the 0.1-s sampling time around 30–35 dB, and then flatten out near the 0.1-s limit at higher values of array loss. The curves of number of fade events for the three-element array all show steeper decrease with array loss (Figure 17) compared to the gentler slopes of the two-element DSS-25/DSS-26 case (Figure 7) and two-element hypothetical (not shown) arrays. Similar behavior of these trends was also observed for the Goldstone hypothetical three-element case, as can be seen from Figure 15.

IV. Conclusions

In this study, we compared average array loss derived from delay RMS over 10-min intervals measured by STIs against instantaneous array loss derived from the STI delay measurements at 0.1-s resolution. We chose the two months having the largest and smallest delay RMS values for two DSN sites, Goldstone and Canberra. These results provided reasonable bounds over the yearly variation in array loss expected for given scenarios. In cases where the average array loss reached its 3-dB limit (for a two-element array), estimates of instantaneous array loss statistics from 0.1-s STI phase observations are preferred. It is expected that the best-case month and worst-case month cumulative distribution curves provide bounds on array loss applicable for any month of the year. We expect that as more years of data are acquired, the bounds will tighten. The previously published average array loss curves should suffice for link studies at 7.15 GHz and are considered conservative for percentiles below ~90 percent.

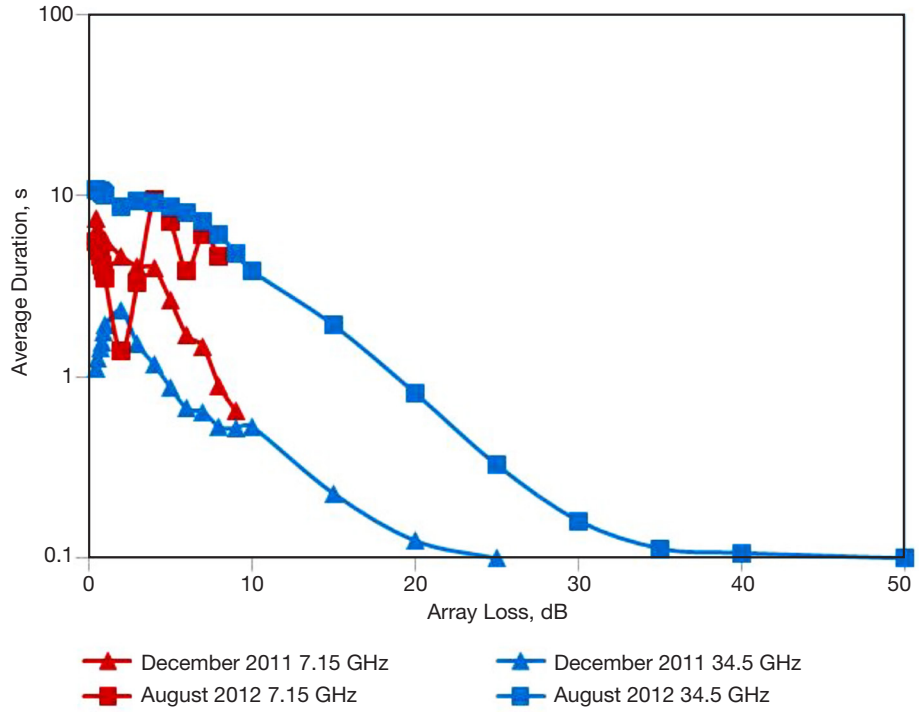

Figure 14. Average duration versus fade threshold for hypothetical three-element array for Goldstone at 47-deg elevation angle for August 2012 and December 2011 at 34.5 GHz (blue curves) and at 7.15 GHz (red curves).

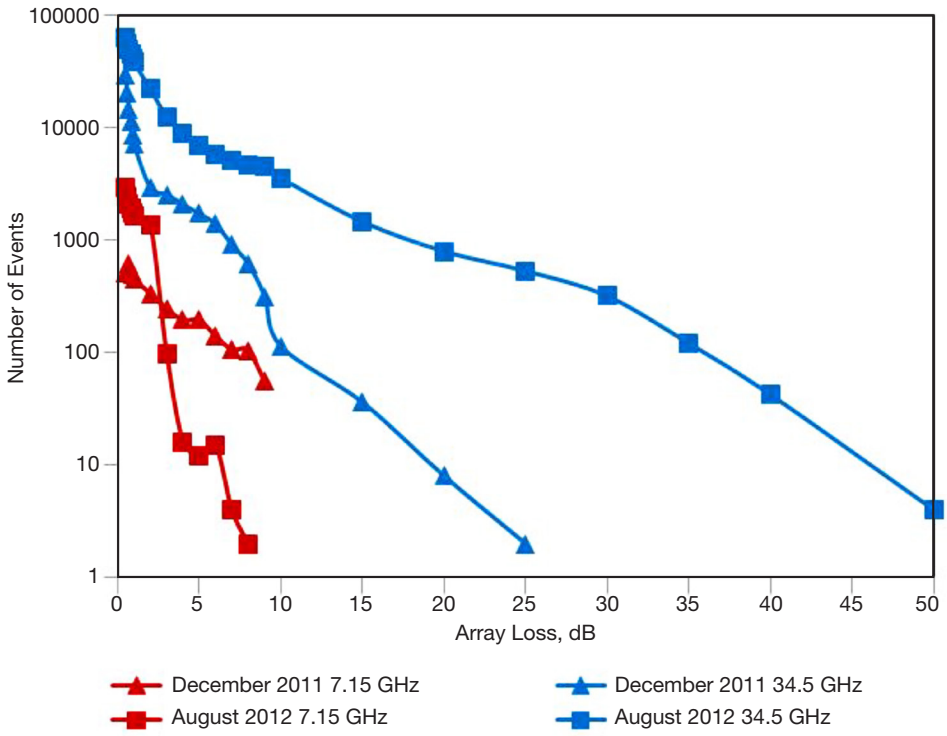

Figure 15. Number of fades versus fade threshold for hypothetical three-element array for Goldstone at 47-deg elevation angle for August 2012 and December 2011 at 34.5 GHz (blue curves) and at 7.15 GHz (red curves).

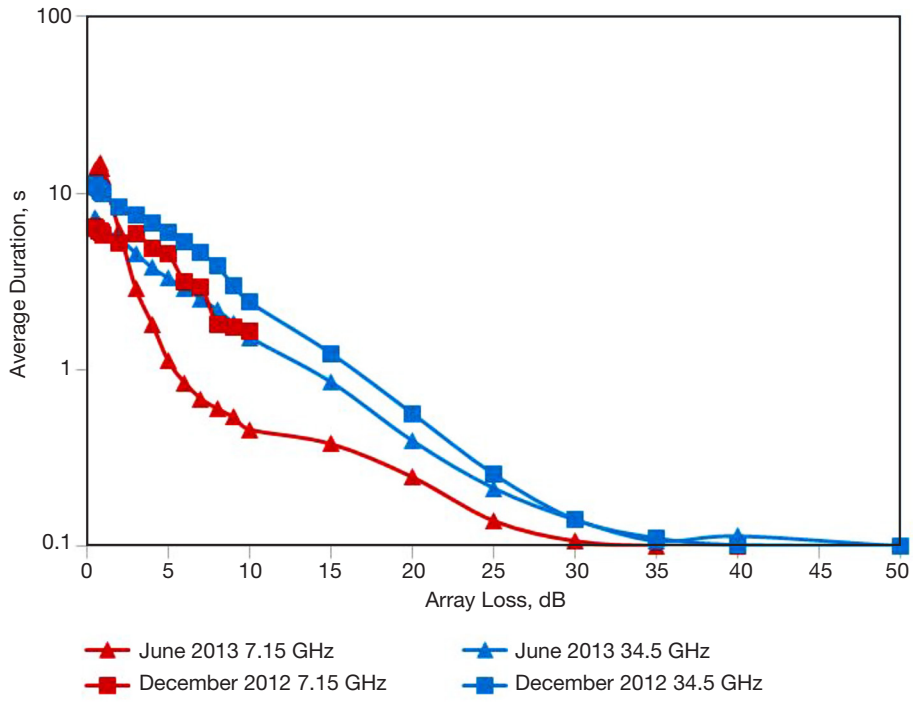

Figure 16. Hypothetical three-element array: Canberra STI average fade duration versus fade threshold for worst-case month (December 2012) and best-case month (June 2013) at 34.5 GHz (blue curves) and at 7.15 GHz (red curves).

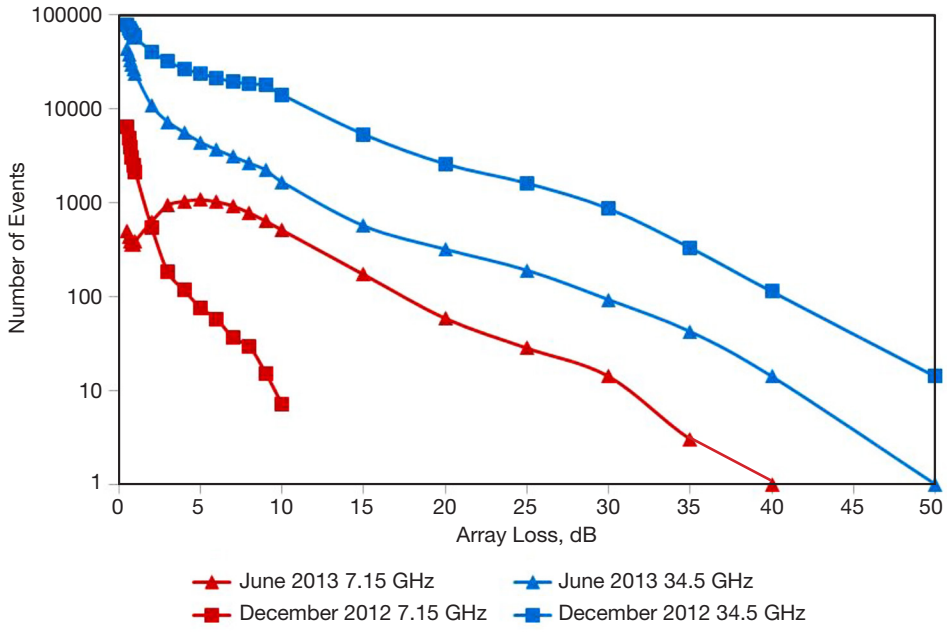

Figure 17. Hypothetical three-element array: Canberra STI number of events exceeding specified fade threshold for worst-case month (December 2012) and best-case month (June 2013) at 34.5 GHz (blue curves) and at 7.15 GHz (red curves).

At 34.5 GHz, where losses are higher, care should be taken to account for the fact that the instantaneous loss is sometimes much larger than the average loss for two-element arrays, especially at high percentiles. The instantaneous array loss curves for best-case month and worst-case month are expected to provide reasonable bounds for given percentiles over all months of a year. Under the same conditions, that probability is substantially reduced for an array of three or more elements.

These studies of average and instantaneous array loss provide sufficient information about atmospheric decorrelation for a flight project to account for this effect in the design of a telecommunications uplink involving two or more arrayed antennas in the DSN. Future studies are being planned to assess the usefulness of applying the average array loss methodology for arrays consisting of a large number of elements.

Acknowledgments

We want to thank Faramaz Davarian, Steven Townes, and Barry Geldzahler for support of this work. We also would like to thank Charles Naudet for providing a detailed review of this article.

References

[1] D. D. Morabito and L. R. D'Addario, "Atmospheric Array Loss Statistics for the Goldstone and Canberra DSN Sites Derived from Site Test Interferometer Data," *The Interplanetary Network Progress Report*, vol. 42-196, Jet Propulsion Laboratory, Pasadena, California, pp. 1–23, February 15, 2014.
http://ipnpr.jpl.nasa.gov/progress_report/42-196/196A.pdf

[2] D. D. Morabito and L. R. D'Addario, "Two-Element Uplink Array Loss Statistics Derived from Site Test Interferometer Phase Data for the Goldstone Climate: Initial Study Results," *The Interplanetary Network Progress Report*, vol. 42-186, Jet Propulsion Laboratory, Pasadena, California, pp. 1–20, August 15, 2011.
http://ipnpr.jpl.nasa.gov/progress_report/42-186/186B.pdf

[3] S. D. Slobin, "Atmospheric and Environmental Effects," *DSN Telecommunications Link Design Handbook*, DSN No. 810-005, Rev. E, Module 105, Rev. D, Jet Propulsion Laboratory, Pasadena, California, September 15, 2009.
http://deepspace.jpl.nasa.gov/dsndocs/810-005/105/105D.pdf

[4] S. D. Slobin, "70-m Subnet Telecommunications Interfaces," *DSN Telecommunications Link Design Handbook*, DSN No. 810-005, Module 101, Rev. D, Jet Propulsion Laboratory, Pasadena, California, April 21, 2011.
http://deepspace.jpl.nasa.gov/dsndocs/810-005/101/101D.pdf

[5] S. D. Slobin, "34-m HEF Subnet Telecommunications Interfaces," *DSN Telecommunications Link Design Handbook*, DSN No. 810-005, Rev. E, Module 103, Rev. B, Jet Propulsion Laboratory, Pasadena, California, September 19, 2008.
http://deepspace.jpl.nasa.gov/dsndocs/810-005/103/103B.pdf

[6] S. D. Slobin, "34-m BWG Stations Telecommunications Interfaces," *DSN Telecommunications Link Design Handbook*, DSN No. 810-005, Module 104, Rev. G, Jet Propulsion Laboratory, Pasadena, California, March 5, 2013.
http://deepspace.jpl.nasa.gov/dsndocs/810-005/104/104G.pdf

[7] D. D. Morabito, L. R. D'Addario, R. J. Acosta, and J. A. Nessel, "Tropospheric Delay Statistics Measured by Two Site Test Interferometers at Goldstone, California," *Radio Science*, vol. 48, no. 6, pp. 729–738, November/December 2013.
http://onlinelibrary.wiley.com/doi/10.1002/2013RS005268/abstract

[8] R. S. Kimberk, T. R. Hunter, P. S. Leiker, R. Blundell, G. U. Nystrom, G. R. Petitpas, J. Test, R. W. Wilson, P. Yamaguchi, and K. H. Young, "A Multi-Baseline 12 GHz Atmospheric Phase Interferometer with One Micron Path Length Sensitivity," *Journal of Astronomical Instrumentation*, vol. 1, no. 1, July 31, 2012.
http://www.worldscientific.com/doi/pdf/10.1142/S225117171250002X

[9] L. R. D'Addario, "Combining Loss of a Transmitting Array due to Phase Errors," *The Interplanetary Network Progress Report*, vol. 42-175, Jet Propulsion Laboratory, Pasadena, California, pp. 1–7, November 15, 2008.
http://ipnpr.jpl.nasa.gov/progress_report/42-175/175G.pdf